Source of Acquisition
NASA Johnson Space Center

A Simplified, Closed-Form Method for Screening Spacecraft Orbital Heating Variations

S. L. Rickman
NASA-Lyndon B. Johnson Space Center, Houston, Texas, 77058

A closed-form analytical technique has been developed to screen orbital average heating variations as a function of beta angle, altitude, surface area, and surface optical properties. Using planetary view factor equations for surfaces parallel-to and normal-to the local vertical, a cylindrical umbral shadow approximation, and a simplified albedo flux model, heating rate equations are formulated and then integrated to obtain orbital average heating. The results are compared to detailed analytical predictions using Monte Carlo integration and an assessment of error is presented.

Nomenclature

A	= flat plate surface area
a	= albedo factor
α	= solar absorptivity
β	= beta angle
ε	= infrared emissivity
h	= circular orbit altitude above planet surface
$\dot{Q}$	= heating rate
$\dot{q}_{PLANET}$	= planetary infrared flux
$\dot{q}_{SOLAR}$	= solar flux
r_e	= planet radius
$\vec{r}$	= spacecraft radius vector
$\hat{s}$	= solar vector
θ	= orbit angle measured from orbit noon
VF	= view factor to planet surface

Sub- and Superscripts

AVG	= orbital average
Z	= zenith (space) facing surface
N	= nadir (planet) facing surface
F	= forward (velocity vector) facing surface
A	= aft facing surface
P	= port facing surface
S	= starboard facing surface
$\parallel$	= surface normal parallel to the local vertical
$\perp$	= surface normal perpendicular to the local vertical

Introduction

Characterization of the on-orbit thermal environment involves orbital parameters such as altitude and beta angle, environmental constants (solar, albedo, and planetary infrared constants), and spacecraft surface optical properties (α and ε). Environmental heating calculations assessing the variation in one or more of these parameters has been relegated to the use of main frame computer analysis codes such as the Thermal Radiation Analyzer System (TRASYS) or Thermal Synthesizer System (TSS). Rickman and Ortiz (Reference 1) developed the Thermal Interactive Mission Evaluation System, which allowed for rapid calculation of simplified on-orbit thermal environments and parametric analyses. Such programs served as screening tools and their use demonstrated a significant reduction in the number of more detailed analyses that would have been required had the screening tool not been available.

A useful screening calculation is presented in this work and can be expressed as a closed form solution given some constraining assumptions. Nevertheless, the described method allows for calculation of detailed environmental heating profiles as a function of orbit angle in addition to integrated orbital average heating rates for individual flux components.

Assumptions

This method described here is applicable given the following assumptions:

a. the central body has a constant infrared flux emission over its entire surface;

b. the albedo factor, a, is assumed constant over the entire surface;

c. the spacecraft is orbiting at a low altitude (i.e., $h << r_e$) and in a circular orbit;

d. the overall spacecraft time constant is on the order of the orbit period;

e. the spacecraft is oriented in a fixed local-vertical local-horizontal attitude with surfaces facing in the principal directions as discussed below.

Assumption (a) is required to simplify the integration of the planetary heating flux and is applicable for Earth-orbiting spacecraft.

For assumption (b), while the abledo factor is constant, the albedo flux varies as the cosine of the orbit angle.

Assumption (c) constrains the analysis to low altitudes in order to allow the simplifying assumption of a cylindrical umbral shadow and a locally constant albedo heating flux. These concepts will be developed in greater detail below.

Assumption (d) validates the use of orbit average heating as a screening tool, however, the expressions established for heating as a function of orbit angle are useful for screening instantaneous heating to surfaces.

Assumption (e) greatly simplifies the view factor analysis since only two types of planetary view factors need be calculated. This assumption, however, limits the applicability of this technique to surfaces facing in the principal directions (i.e., forward-, aft-, starboard-, port-, zenith- and nadir-facing surfaces).

General Expressions

Consider a spacecraft in a low altitude, orbit about a planet as presented in Fig. 1. Due to precession of the orbit plane and the planet's motion about the sun, the angle, β, between the solar vector, $\hat{s}$, and its projection onto the orbit plane will vary as a function of time.

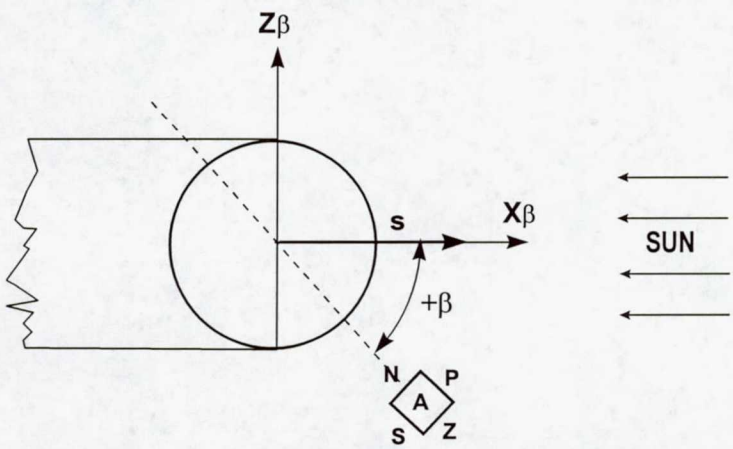

Fig. 1 Problem geometry and β definition.

As β varies, so too will the fraction of the orbit in which the spacecraft spends in the planet's umbral shadow. At Earth's distance from the sun, the umbral shadow cone stretches over 800,000 miles into space. Hence, the shadow cone is nearly cylindrical in shape close to Earth and deviates by only about 0.26° from the assumed cylindrical shadow. With this simplification, an expression relating the terminator entry and exit angles, θ_{ENTRY} and θ_{EXIT}, respectively, with β is easily obtained. This simplifying assumption does not provide for the transition through the penumbra. At low altitudes, however, this does not pose a problem as the time spent in the penumbra is measured in seconds compared to an orbit period on the order of 1.5 hours.

As depicted in Fig. 2, the position of the spacecraft, $\vec{r}$, can be expressed as a function of the altitude above the planet, *h*, the radius of the planet, r_e, the angle from orbit noon, θ, and β:

$$\vec{r} = (r_e + h)\cos\theta\cos\beta\hat{i} + (r_e + h)\sin\theta\hat{j} + (r_e + h)\cos\theta\sin\beta\hat{k} \tag{1}$$

The projection of this vector onto the $Y_\beta Z_\beta$-plane is:

$$\vec{r}' = (r_e + h)\sin\theta\hat{j} + (r_e + h)\cos\theta\sin\beta\hat{k} \tag{2}$$

And the magnitude of the projection is simply:

$$|\vec{r}'| = (r_e + h)\sqrt{\sin^2\theta + \cos^2\theta \sin^2\beta} \tag{3}$$

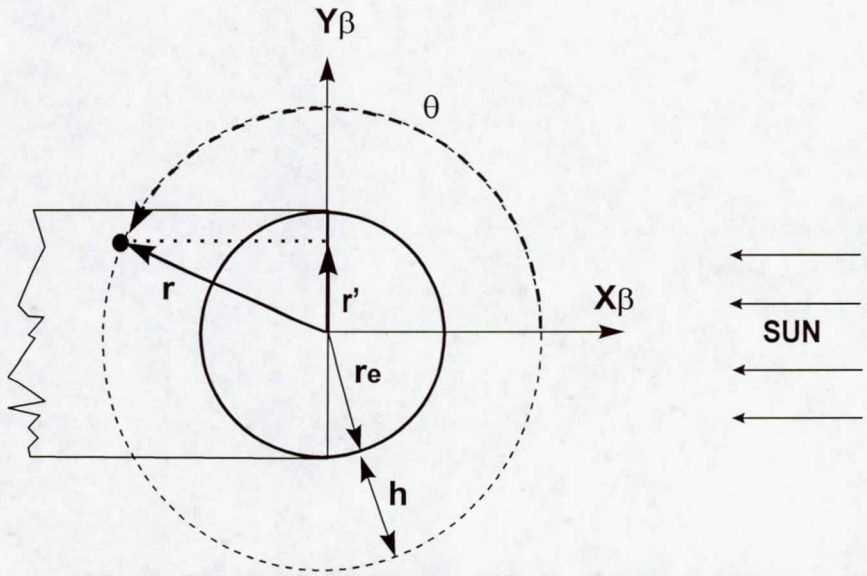

Fig. 2 Geometry of the simplified eclipse problem.

Examination of the geometry reveals that the onset of the umbral shadowing occurs when the magnitude of $\vec{r}'$ is less than r_e, or:

$$\sin\theta \le \sqrt{\frac{1}{\cos^2\beta}\left[\left(\frac{r_e}{r_e + h}\right)^2 - \sin^2\beta\right]} \tag{4}$$

Since sin θ is defined between -π/2 and +π/2, we note that $\theta_{ENTRY} = \pi - \theta$ and $\theta_{EXIT} = \pi + \theta$.

The heating incident on an orbiting flat plate varies as a function of the orbit angle, θ, and is given by:

$$\dot{Q}_{TOTAL}^{PLATE}(\theta) = \dot{Q}_{SOLAR}^{PLATE}(\theta) + \dot{Q}_{ALBEDO}^{PLATE}(\theta) + \dot{Q}_{PLANET}^{PLATE}(\theta) \tag{5}$$

For six plates, arranged as shown in Fig. 2, the total absorbed heating as a function of θ is given by:

$$\dot{Q}_{TOTAL}(\theta) = \sum_{m=Z,N,F,A,P,S} \dot{Q}_{SOLAR}^{m}(\theta) + \sum_{m=Z,N,F,A,P,S} \dot{Q}_{ALBEDO}^{m}(\theta) + \sum_{m=Z,N,F,A,P,S} \dot{Q}_{PLANET}^{m}(\theta) \tag{6}$$

where the superscripts Z, N, F, A, P, and S refer to the zenith-, nadir-, forward-, aft-, port-, and starboard-facing plates, respectively.

View factor calculations are required in order to determine the amount of planetary infrared and albedo fluxes impinging on the analytical surfaces. Reference 2 provides a thorough discussion of planetary- and albedo-radiation view factor calculations for a planet-oriented and arbitrarily-oriented flat panel. However, the treatment presented herein is restricted to surfaces oriented normal-to or parallel-to the nadir direction with the further restriction that $h << r_e$. Reference 3 provides the general derivation of the planetary view factor for a flat plate surface and has been adapted, here, for the special cases of plates whose surface normals are parallel (nadir-facing) to and perpendicular (forward-, aft-, port-, and starboard-facing) to the local vertical vector, respectively:

$$(VF)_{\parallel} = \left(\frac{r_e}{r_e + h}\right)^2 \tag{7}$$

$$(VF)_{\perp} = \left(\frac{1}{2\pi}\right)\left[\pi - 2\sin^{-1}\left(\sqrt{1-\left(\frac{r_e}{r_e+h}\right)^2}\right) - \sin\left(2\sin^{-1}\left(\sqrt{1-\left(\frac{r_e}{r_e+h}\right)^2}\right)\right)\right] \tag{8}$$

Note, also, that since the zenith facing surface cannot view the planet:

$$(VF)_{ZENITH} = 0 \tag{9}$$

Solar Heating

The orbital average absorbed solar heating is obtained by direct integration of the instantaneous solar heating equations over the applicable angles and dividing by the angular span of an entire orbit (2π). For orbits that pass into the planet's umbral shadow, i.e., when:

$$\left(\sqrt{\left(\frac{r_e}{r_e+h}\right)^2 - \sin^2\beta}\right) > 0 \tag{10}$$

the integrals are:

$$\left(\dot{Q}_{SOLAR}\right)_{AVG}^{Z} = \frac{\dot{q}_{SOLAR}\alpha_Z A_Z \cos\beta}{2\pi}\int_{-\pi/2}^{+\pi/2}\cos\theta d\theta \tag{11}$$

$$\left(\dot{Q}_{SOLAR}\right)_{AVG}^{N} = \frac{-\dot{q}_{SOLAR}\alpha_N A_N \cos\beta}{2\pi}\int_{+\pi/2}^{\theta_{ENTRY}}\cos\theta d\theta - \frac{\dot{q}_{SOLAR}\alpha_N A_N \cos\beta}{2\pi}\int_{\theta_{EXIT}}^{-\pi/2}\cos\theta d\theta \tag{12}$$

$$\left(\dot{Q}_{SOLAR}\right)_{AVG}^{F} = \frac{-\dot{q}_{SOLAR}\alpha_F A_F \cos\beta}{2\pi}\int_{\theta_{EXIT}}^{+2\pi}\sin\theta d\theta \tag{13}$$

$$\left(\dot{Q}_{SOLAR}\right)_{AVG}^{A} = \frac{\dot{q}_{SOLAR}\alpha_A A_A \cos\beta}{2\pi}\int_{0}^{\theta_{ENTRY}}\sin\theta d\theta \tag{14}$$

For $\beta \geq 0$:

$$\left(\dot{Q}_{SOLAR}\right)_{AVG}^{P} = \frac{\dot{q}_{SOLAR}\alpha_P A_P \sin\beta}{2\pi}\int_{\theta_{EXIT}}^{\theta_{ENTRY}} d\theta \tag{15}$$

$$\left(\dot{Q}_{SOLAR}\right)_{AVG}^{S} = 0 \tag{16}$$

For $\beta < 0$:

$$\left(\dot{Q}_{SOLAR}\right)_{AVG}^{P} = 0 \tag{17}$$

$$\left(\dot{Q}_{SOLAR}\right)_{AVG}^{S} = \frac{-\dot{q}_{SOLAR}\alpha_S A_S \sin\beta}{2\pi}\int_{\theta_{EXIT}}^{\theta_{ENTRY}} d\theta \tag{18}$$

and for orbits that experience no eclipse, the limits of integration θ_{ENTRY} and θ_{EXIT} given above may be replaced by $+\pi$ and $-\pi$, respectively.

A Simplified Albedo Model

A true albedo model would account for variations in the albedo constant as a function of solar incidence angle as well as variations in the view factor to a surface with varying flux intensity. The effect of the latter of these two factors is most evident near the ground terminators where the slope of the cosine reduction in solar flux on the planet's surface is greatest. For low altitude orbits, however, it is assumed that only a small portion of the planet is visible and that any local variation in albedo flux intensity is small. As an example, at 220 nm altitude, the distance to the horizon is approximately 1200 nm. At a β of $\pi/2$ (i.e, 90°), the spacecraft is orbiting along the ground terminator with a view subtending 0.35 radians in all directions. Assuming a pure cosine reduction in the albedo flux, the maximum intensity of the albedo flux, at the extent of the view, is approximately 34% of that at the subsolar point. Since half of the plate is viewing a darkened planet, an upper limit of about half that value, or 17%, of the subsolar albedo flux is assumed in the worst case. Since the visible portion of the planet's surface is not uniformly lit (with the albedo flux going to zero at the ground terminator) a more realistic estimate of the albedo error in this extreme case is closer to 10%. It should be noted that analyses performed at lower values of β will exhibit less error since little time is spent at or near the ground terminators. At the subsolar point, the variation over the fraction of the visible illuminated surface is, at most, about 6%.

With the inherent error in hand, then, the simplified orbital average albedo heating can be expressed as the sum of the integrals over the illuminated portion of the orbit ($-\pi/2 \leq \theta \leq +\pi/2$) divided by angular span of the entire orbit (2π):

$$\left(\dot{Q}_{ALBEDO}\right)_{AVG}^{Z} = 0 \tag{19}$$

$$\left(\dot{Q}_{ALBEDO}\right)_{AVG}^{N} = \frac{a(VF)_{\parallel}\dot{q}_{SOLAR}\alpha_N A_N \cos\beta}{2\pi}\int_{-\pi/2}^{+\pi/2}\cos\theta d\theta \tag{20}$$

$$\left(\dot{Q}_{ALBEDO}\right)_{AVG}^{F} = \frac{a(VF)_{\perp}\dot{q}_{SOLAR}\alpha_F A_F \cos\beta}{2\pi}\int_{-\pi/2}^{+\pi/2}\cos\theta d\theta \tag{21}$$

$$\left(\dot{Q}_{ALBEDO}\right)_{AVG}^{A} = \frac{a(VF)_{\perp}\dot{q}_{SOLAR}\alpha_A A_A \cos\beta}{2\pi}\int_{-\pi/2}^{+\pi/2}\cos\theta d\theta \tag{22}$$

$$\left(\dot{Q}_{ALBEDO}\right)_{AVG}^{P} = \frac{a(VF)_{\perp}\dot{q}_{SOLAR}\alpha_P A_P \cos\beta}{2\pi}\int_{-\pi/2}^{+\pi/2}\cos\theta d\theta \tag{23}$$

$$\left(\dot{Q}_{ALBEDO}\right)_{AVG}^{S} = \frac{a(VF)_{\perp}\dot{q}_{SOLAR}\alpha_S A_S \cos\beta}{2\pi}\int_{-\pi/2}^{+\pi/2}\cos\theta d\theta \tag{24}$$

Planetary Infrared Heating

The planetary infrared heating is easily calculated due to the assumption of uniform flux emission over the entire planet. Due to the constant planetary infrared heating assumption, the orbital average planetary infrared heating is not a function of θ and is given by:

$$\left(\dot{Q}_{PLANET}\right)_{AVG}^{Z} = 0 \tag{25}$$

$$\left(\dot{Q}_{PLANET}\right)_{AVG}^{N} = (VF)_{\parallel}\dot{q}_{PLANET}\varepsilon_N A_N \tag{26}$$

$$\left(\dot{Q}_{PLANET}\right)_{AVG}^{F} = (VF)_{\perp}\dot{q}_{PLANET}\varepsilon_F A_F \tag{27}$$

$$\left(\dot{Q}_{PLANET}\right)_{AVG}^{A} = (VF)_{\perp}\dot{q}_{PLANET}\varepsilon_A A_A \tag{28}$$

$$\left(\dot{Q}_{PLANET}\right)_{AVG}^{P} = (VF)_{\perp}\dot{q}_{PLANET}\varepsilon_P A_P \tag{29}$$

$$\left(\dot{Q}_{PLANET}\right)_{AVG}^{S} = (VF)_{\perp}\dot{q}_{PLANET}\varepsilon_S A_S \tag{30}$$

Results

The equations presented above are integrated and the results are presented on a component-by-component basis.

For the solar heating where an eclipse occurs:

$$\left(\dot{Q}_{SOLAR}\right)_{AVG}^{Z} = \left(\frac{1}{\pi}\right)\dot{q}_{SOLAR}\alpha_Z A_Z \cos\beta \tag{31}$$

$$\left(\dot{Q}_{SOLAR}\right)_{AVG}^{N} = -\left(\frac{1}{\pi}\right)\dot{q}_{SOLAR}\alpha_N A_N \cos\beta\left(\frac{1}{\cos\beta}\sqrt{\left[\left(\frac{r_e}{r_e+h}\right)^2 - \sin^2\beta\right]} - 1\right) \tag{32}$$

$$\left(\dot{Q}_{SOLAR}\right)_{AVG}^{F} = -\left(\frac{1}{2\pi}\right)\dot{q}_{SOLAR}\alpha_F A_F \cos\beta\left[1-\cos\left(\pi-\sin^{-1}\left(\frac{1}{\cos\beta}\sqrt{\left(\frac{r_e}{r_e+h}\right)^2-\sin^2\beta}\right)\right)\right] \tag{33}$$

$$\left(\dot{Q}_{SOLAR}\right)_{AVG}^{A} = -\left(\frac{1}{2\pi}\right)\dot{q}_{SOLAR}\alpha_A A_A \cos\beta\left[1-\cos\left(\pi-\sin^{-1}\left(\frac{1}{\cos\beta}\sqrt{\left(\frac{r_e}{r_e+h}\right)^2-\sin^2\beta}\right)\right)\right] \tag{34}$$

For $\beta \geq 0$:

$$\left(\dot{Q}_{SOLAR}\right)_{AVG}^{P} = \left(\frac{1}{\pi}\right)\dot{q}_{SOLAR}\alpha_P A_P \sin\beta \sin^{-1}\left(\frac{1}{\cos\beta}\sqrt{\left(\frac{r_e}{r_e+h}\right)^2-\sin^2\beta}\right) \tag{35}$$

$$\left(\dot{Q}_{SOLAR}\right)_{AVG}^{S} = 0 \tag{36}$$

For $\beta < 0$:

$$\left(\dot{Q}_{SOLAR}\right)_{AVG}^{P} = 0 \tag{37}$$

$$\left(\dot{Q}_{SOLAR}\right)_{AVG}^{S} = -\left(\frac{1}{\pi}\right)\dot{q}_{SOLAR}\alpha_S A_S \sin\beta \sin^{-1}\left(\frac{1}{\cos\beta}\sqrt{\left(\frac{r_e}{r_e+h}\right)^2-\sin^2\beta}\right) \tag{38}$$

and for the condition when no eclipse occurs, the integral for the zenith surface remains the same and the other surfaces become:

$$\left(\dot{Q}_{SOLAR}\right)_{AVG}^{N} = \left(\frac{1}{\pi}\right)\dot{q}_{SOLAR}\alpha_N A_N \cos\beta \tag{39}$$

$$\left(\dot{Q}_{SOLAR}\right)_{AVG}^{F} = \left(\frac{1}{\pi}\right)\dot{q}_{SOLAR}\alpha_F A_F \cos\beta \tag{40}$$

$$\left(\dot{Q}_{SOLAR}\right)_{AVG}^{A} = \left(\frac{1}{\pi}\right)\dot{q}_{SOLAR}\alpha_A A_A \cos\beta \tag{41}$$

For $\beta \geq 0$:

$$\left(\dot{Q}_{SOLAR}\right)_{AVG}^{P} = \dot{q}_{SOLAR}\alpha_P A_P \sin\beta \tag{42}$$

$$\left(\dot{Q}_{SOLAR}\right)_{AVG}^{S} = 0 \tag{43}$$

For $\beta < 0$:

$$\left(\dot{Q}_{SOLAR}\right)_{AVG}^{P} = 0 \tag{44}$$

$$\left(\dot{Q}_{SOLAR}\right)_{AVG}^{S} = -\dot{q}_{SOLAR}\alpha_S A_S \sin\beta \tag{45}$$

For the albedo heating:

$$\left(\dot{Q}_{ALBEDO}\right)_{AVG}^{Z} = 0 \tag{46}$$

$$\left(\dot{Q}_{ALBEDO}\right)_{AVG}^{N} = \left(\frac{1}{\pi}\right)\dot{q}_{SOLAR}\, a\alpha_N A_N \left(\frac{r_e}{r_e+h}\right)^2 \cos\beta \tag{47}$$

$$\left(\dot{Q}_{ALBEDO}\right)_{AVG}^{F} = \left(\frac{1}{2\pi^2}\right)\dot{q}_{SOLAR}\, a\alpha_F A_F \left[\pi - 2\sin^{-1}\left(\sqrt{1-\left(\frac{r_e}{r_e+h}\right)^2}\right) - \sin\left(2\sin^{-1}\left(\sqrt{1-\left(\frac{r_e}{r_e+h}\right)^2}\right)\right)\right]\cos\beta \tag{48}$$

$$\left(\dot{Q}_{ALBEDO}\right)_{AVG}^{A} = \left(\frac{1}{2\pi^2}\right)\dot{q}_{SOLAR}\, a\alpha_A A_A \left[\pi - 2\sin^{-1}\left(\sqrt{1-\left(\frac{r_e}{r_e+h}\right)^2}\right) - \sin\left(2\sin^{-1}\left(\sqrt{1-\left(\frac{r_e}{r_e+h}\right)^2}\right)\right)\right]\cos\beta \tag{49}$$

$$\left(\dot{Q}_{ALBEDO}\right)_{AVG}^{P} = \left(\frac{1}{2\pi^2}\right)\dot{q}_{SOLAR}\, a\alpha_P A_P \left[\pi - 2\sin^{-1}\left(\sqrt{1-\left(\frac{r_e}{r_e+h}\right)^2}\right) - \sin\left(2\sin^{-1}\left(\sqrt{1-\left(\frac{r_e}{r_e+h}\right)^2}\right)\right)\right]\cos\beta \tag{50}$$

$$\left(\dot{Q}_{ALBEDO}\right)_{AVG}^{S} = \left(\frac{1}{2\pi^2}\right)\dot{q}_{SOLAR}\, a\alpha_S A_S \left[\pi - 2\sin^{-1}\left(\sqrt{1-\left(\frac{r_e}{r_e+h}\right)^2}\right) - \sin\left(2\sin^{-1}\left(\sqrt{1-\left(\frac{r_e}{r_e+h}\right)^2}\right)\right)\right]\cos\beta \tag{51}$$

And, finally, for the planetary infrared heating:

$$\left(\dot{Q}_{PLANET}\right)_{AVG}^{Z} = 0 \tag{52}$$

$$\left(\dot{Q}_{PLANET}\right)_{AVG}^{N} = \dot{q}_{PLANET}\,\varepsilon_N A_N \left(\frac{r_e}{r_e+h}\right)^2 \tag{53}$$

$$\left(\dot{Q}_{PLANET}\right)_{AVG}^{F} = \dot{q}_{PLANET}\,\varepsilon_F A_F \left(\frac{1}{2\pi}\right)\left[\pi - 2\sin^{-1}\left(\sqrt{1-\left(\frac{r_e}{r_e+h}\right)^2}\right) - \sin\left(2\sin^{-1}\left(\sqrt{1-\left(\frac{r_e}{r_e+h}\right)^2}\right)\right)\right] \tag{54}$$

$$\left(\dot{Q}_{PLANET}\right)_{AVG}^{A} = \dot{q}_{PLANET}\,\varepsilon_A A_A \left(\frac{1}{2\pi}\right)\left[\pi - 2\sin^{-1}\left(\sqrt{1-\left(\frac{r_e}{r_e+h}\right)^2}\right) - \sin\left(2\sin^{-1}\left(\sqrt{1-\left(\frac{r_e}{r_e+h}\right)^2}\right)\right)\right] \tag{55}$$

$$\left(\dot{Q}_{PLANET}\right)_{AVG}^{P} = \dot{q}_{PLANET}\,\varepsilon_P A_P \left(\frac{1}{2\pi}\right)\left[\pi - 2\sin^{-1}\left(\sqrt{1-\left(\frac{r_e}{r_e+h}\right)^2}\right) - \sin\left(2\sin^{-1}\left(\sqrt{1-\left(\frac{r_e}{r_e+h}\right)^2}\right)\right)\right] \tag{56}$$

$$\left(\dot{Q}_{PLANET}\right)_{AVG}^{S} = \dot{q}_{PLANET}\,\varepsilon_S A_S \left(\frac{1}{2\pi}\right)\left[\pi - 2\sin^{-1}\left(\sqrt{1-\left(\frac{r_e}{r_e+h}\right)^2}\right) - \sin\left(2\sin^{-1}\left(\sqrt{1-\left(\frac{r_e}{r_e+h}\right)^2}\right)\right)\right] \tag{57}$$

In order to test the method, a sample case was developed and compared to detailed Monte Carlo predicted heating rates calculated using the Thermal Synthesizer System Heatrate application (Reference 4). The simple geometry of a unit box (1 ft x 1 ft x 1 ft) with optical properties for all box sides set to α=1 and ε=1 was selected so as not to improperly bias the results away from a given viewing direction and heating component with smaller inherent error. The box was assumed to orbit the Earth at an altitude of

220 nm inclined 67° with respect to the equator and would experience the entire range of possible β angles. The solar flux, albedo factor, and planetary infrared flux were assumed to be 443.7 Btu/hr ft^2, 0.3, and 77.0 Btu/hr ft^2, respectively; all well within the accepted ranges (Reference 5). Detailed Monte Carlo analyses were performed for a range of β using 10000 rays per surface for each heating component. A comparison of the orbital average heating resulting from both methods is presented in Fig. 3 with error presented in Table 1.

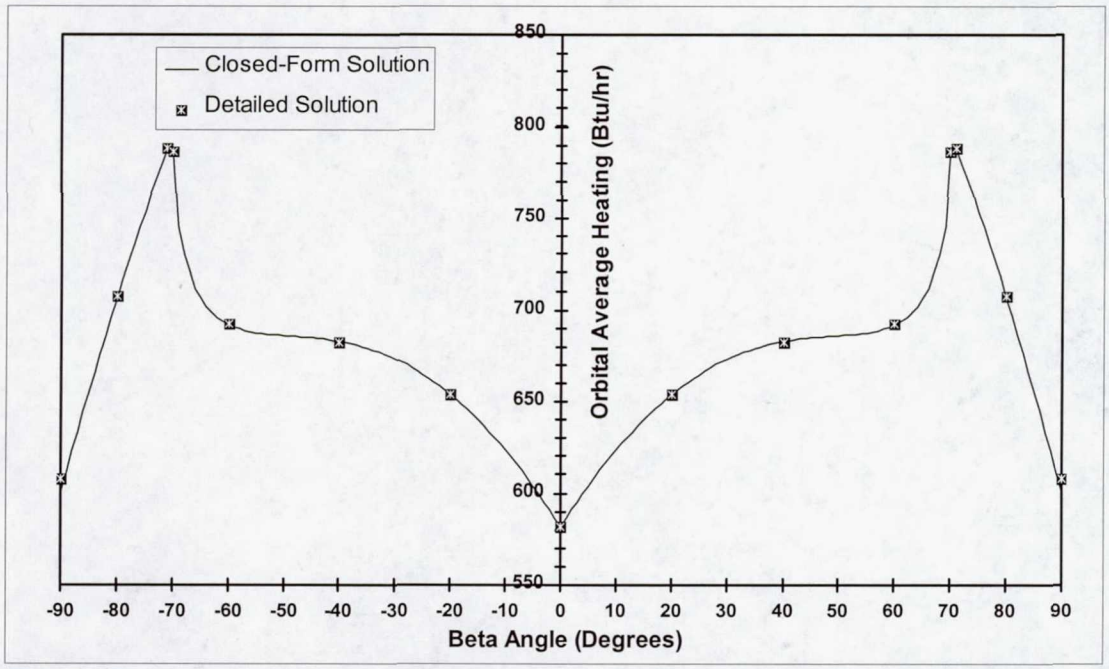

Fig. 3 Comparison of simplified screening technique and detailed Monte Carlo predicted average heating for an orbiting box at 220 nm altitude.

Beta (deg)	Closed-Form Solution (Btu/hr)	Detailed Solution (Btu/hr)	% Error [100 x (Detailed - Closed)/Detailed]
-90	600.1	607.4	1.2
-80	706.4	707.8	0.2
-71	787.9	788.6	0.1
-70	784.2	786.5	0.3
-60	691.9	692.3	0.1
-40	682.8	682.6	0.0
-20	653.9	654.2	0.1
0	581.7	581.9	0.0
20	653.9	654.2	0.1
40	682.8	682.6	0.0
60	691.9	692.3	0.1
70	784.2	786.5	0.3
71	787.9	788.6	0.1
80	706.4	707.8	0.2
90	600.1	607.4	1.2

Table 1 Tabular results and a comparison of the detailed and closed-form solution error.

Examination of the results indicates that the simplified method produces exceptionally good results when compared with the detailed predictions. Errors on the order of 1% are observed at $\beta = 90°$ with much lower error at lower values of β. These errors are well within the statistical error observed in the detailed Monte Carlo analysis results.

Potential Applications

The method appears to be well suited for screening where approximate solutions will suffice. Establishing the worst-case hot and cold orbits prior to a more detailed analysis has the potential to significantly reduce the magnitude of the overall thermal analysis cycle. If implemented in spreadsheet form, engineers can rapidly investigate the effects of optical property degradation, altitude and beta angle variations. Expressions for heating as a function of orbit angle are useful for studies of instantaneous orbit heating. Such an algorithm may also have application as a screening tool in a larger analysis system and would promote the development of an "intelligent system" to pre-select analysis cases.

Concluding Remarks

A simplified, closed-form method for screening orbital heating variations as a function of the β, altitude, surface area, and optical properties has been developed and compared to detailed analytical predictions. The method is easily implemented in computerized spreadsheet programs and provides a rapid assessment of orbital heating trends, identifies maximum and minimum overall heating conditions, and allows exploration of the sensitivity of the spacecraft absorbed heating characteristics through variation of design parameters such as optical properties and areas. Implementation of this method may prove useful as a screening tool for spacecraft thermal engineers prior to the initiation of detailed orbital heating analyses.

References

1. Rickman, S. L. and Ortiz, C. R., Thermal Interactive Mission Evaluation System (TIMES), Version 1.0, JSC-22332, 1986.

2. Furukawa, M., "Practical Method for Calculating Radiation Incident Upon a Panel in Orbit," Journal of Thermophysics and Heat Transfer, Vol. 6, Number 1, 1992, pp. 173-177.

3. Ballinger, J. C., Elizalde, J. C., Garcia-Varela, R. M., and Christiansen, E. H., Environmental Control of Space Vehicles, Part II, Thermal Environment of Space, Convair, ERR-AN-016, 1960.

4. User Manual, Thermal Synthesizer System, Release 9.01, LMSMSS-31078, Revision D., 1999.

5. Gilmore, D. G. (Editor), Satellite Thermal Control Handbook, El Segundo, The Aerospace Corporation, 1994.